



---

# **NRC - CNRC**

---

## **Predicting the fire resistance behaviour of high strength concrete columns**

**Kodur, V.K.R.; Wang, T.C.; Cheng, F.P.**

**NRCC-43379**

**A version of this document is published in / Une version de ce document se trouve dans :  
Cement and Concrete Composites, v. 26, no. 2, Feb. 2004, pp. 141-153**

<http://irc.nrc-cnrc.gc.ca/ircpubs>



# PREDICTING THE FIRE RESISTANCE BEHAVIOUR OF HIGH STRENGTH CONCRETE COLUMNS

by V.K.R Kodur<sup>1</sup>, T.C. Wang<sup>2</sup> and F.P. Cheng<sup>3</sup>

## ABSTRACT

A numerical model, in the form of a computer program, for tracing the behaviour of high performance concrete (HPC) columns exposed to fire is presented. The three stages, associated with the thermal and structural analysis, for the calculation of fire resistance of columns are explained. A simplified approach is proposed to account for spalling under fire conditions. The use of the computer program for tracing the response of an HPC column from the initial pre-loading stage to collapse, due to fire, is demonstrated.

The validity of the numerical model used in the program is established by comparing the predictions from the computer program with results from full-scale fire resistance tests. Details of fire resistance experiments carried out on HPC columns, together with results, are presented. The computer program can be used to predict the fire resistance of HPC columns for any value of the significant parameters, such as load, section dimensions, fiber reinforcement, column length, concrete strength, aggregate type, and fiber reinforcement.

**KEYWORDS:** Fire resistance, computer program, high temperature, high performance concrete columns, spalling, numerical model

## INTRODUCTION

In recent years, the construction industry has shown significant interest in the use of high performance concrete (HPC). This is due to improvements in structural performance, such as high strength and durability, that it can provide compared to traditional, normal strength concrete (NSC). Generally, concrete up to a compressive strength of 55 MPa is referred to as normal strength concrete (NSC), while concrete with compressive strength in excess of 55 MPa is classified as high strength concrete (HSC). HPC is typically characterized by high strength, good workability and durability and HSC is a subset of HPC.

One of the major uses of HPC in buildings is for reinforced concrete (RC) columns. The columns form the main load bearing components in a building and hence, the provision of appropriate fire safety measures is one of the major safety requirements in building design [1]. However, most concrete design standards have no guidelines for the fire resistance design of RC columns made of HPC [2,3].

Further, results of fire tests in a number of laboratories have shown that there are well-defined differences between the properties of HSC and NSC at elevated temperatures [4,5]. Also, concern has developed regarding the occurrence of explosive spalling when HSC is subjected to rapid heating, as in the case of a fire [4,5,6].

---

<sup>1</sup> Senior Research Officer, Inst. for Res. in Constr., National Research Council, Ottawa, ON, Canada. E-mail: Venkatesh.kodur@nrc.ca

<sup>2</sup> Ph. D. Student, Department of Civil Engineering, National Chiao Tung University, HsinChu, Taiwan.

<sup>3</sup> Associate Prof., Department of Civil Engineering, National Chiao Tung University, HsinChu, Taiwan.

Recent developments, including the development of numerical techniques and an enhanced knowledge of the thermal and mechanical properties of materials at elevated temperatures, have made it possible to determine the fire resistance of various structural members by calculation. A detailed literature review revealed that while computer models have been established for determining the fire resistance of NSC columns, this is not the case with HPC columns [6,7]. Further, there is only limited test data available on the fire resistance of HPC columns [5,7].

To develop guidelines for the fire resistant design and for the construction of HPC columns, a collaborative research project was undertaken between National Research Council of Canada (NRCC) and National Chiao Tung University (NCTU), Taiwan. Both experimental and theoretical studies were carried out to investigate the fire performance of HPC columns.

In this paper, a numerical model in the form of a computer program, for evaluating the fire resistance of HPC columns, is presented. Spalling of HSC, under fire conditions, is accounted for in the model through a simplified approach. Results of experiments are used to trace the structural behavior of HPC concrete columns at elevated temperatures. The validity of the numerical model used in the program is established by comparing the predictions from the computer program with results from full-scale fire resistance tests.

## **RESEARCH SIGNIFICANCE**

When used in buildings, structural members must be designed to satisfy appropriate fire resistance requirements in addition to load carrying requirements. These fire resistance requirements can be attributed to the fact that, when other measures of controlling the fire fail, structural integrity is the last line of defense.

Generally, concrete structural members exhibit good performance under fire situations. Studies show, however, that the fire performance of HSC is different from that of NSC and may not exhibit good performance in fire. Furthermore, the spalling of concrete under fire conditions is one of the major concerns due to the low water-binder ratio in HSC. The spalling of concrete exposed to fire has been observed under laboratory and real fire conditions [5,6,8]. Spalling, which results in the rapid loss of concrete during a fire, exposes deeper layers of concrete to fire temperatures, thereby increasing the rate of transmission of heat to the inner layers of the member and to the reinforcement.

Spalling is theorized to be caused by the build-up of pore pressure during heating [4,8]. HSC is believed to be more susceptible to this pressure build-up because of its low permeability compared to NSC. The extremely high water vapor pressure, generated during exposure to fire, cannot escape due to the high density of HSC and this pressure often reaches the saturation vapor pressure. At 300°C, the pressure reaches about 8 MPa. Such internal pressures are often too high to be resisted by the HSC mix having a tensile strength of about 5 MPa [4]. Data from various studies show that predicting fire performance of HSC, in general, and spalling, in particular, is very complex since it is affected by a number of factors [4,5,8].

This paper describes the development and validation of a computer program for evaluating fire resistance of HPC columns.

## **EXPERIMENTAL STUDIES**

## Test Specimens

The experimental study consisted of fire resistance tests on fifteen reinforced concrete columns, with various parameters. Of these experiments four HPC columns, namely THC4, THC8, THS11 and THP14, were selected for detailed validation of the computer program. All columns were 3810 mm long and of a square cross-section of 305 mm. The dimensions of the column cross-section and other specifics of the columns are given in Table 1.

**Table 1 - Summary of Test Parameters and Results for HPC Columns**

| Column  | Column Dimensions (mm) | Concrete Strength (f'c) |                | Factored Resistance (Cr) (kN) | Test Load (C) (kN) | Load Intensity (C/Cr) | Fire Resistance |               |
|---------|------------------------|-------------------------|----------------|-------------------------------|--------------------|-----------------------|-----------------|---------------|
|         |                        | 28 day (MPa)            | test day (MPa) |                               |                    |                       | Test (h:min)    | Model (h:min) |
| THC4    | 305 x 305              | 60.6                    | 99.6           | 3697                          | 2000               | 0.54                  | 3:22            | 3:06          |
| THC8    | 305 x 305              | 60.4                    | 72.7           | 2805                          | 2000               | 0.71                  | 5:05            | 4:31          |
| THS11*  | 305 x 305              | 63.2                    | 89.1           | 3349                          | 2200               | 0.66                  | 3:26            | 2:56          |
| THP14** | 305 x 305              | 51.9                    | 86.8           | 3266                          | 2200               | 0.67                  | 3:53            | 3:03          |

\* Contained steel fibers

\*\* Contained polypropylene fibers

The columns were designed in accordance with ACI specifications [3]. All columns had four, 25 mm, longitudinal bars and these main bars were welded to the end plates. The bars were tied with 10 mm ties at a spacing of 75 mm at both ends and 145 mm in the middle. The main reinforcing bars and ties had a specified yield strength of 420 MPa and 280 MPa, respectively. Figure 1 shows the elevation and cross-sectional details of the columns together with the locations of the ties.

Four batches of concrete were used in fabricating the columns. Steel and polypropylene fibers reinforcement were added to Batch 3 and Batch 4, respectively. The coarse aggregate in Batch 2 was of carbonate type, while the other batches were made with siliceous aggregate. Columns THC4, THC8, THS11 and THP14 were fabricated from Batch 1, Batch 2, Batch 3 and Batch 4, respectively. All four batches of concrete were made with general purpose Type 1 Portland cement.

The average compressive cylinder strength of the concrete, measured 28 days after pouring and on the day of testing, are given in Table 1. The moisture condition at the center of the column was also measured on the day of the test, by inserting a Vaisala moisture sensor into a hole drilled in the concrete. The moisture conditions of Columns THC4, THC8, THS11 and THP14 are approximately equivalent to those in equilibrium with air of 78%, 67%, 99% and 85% relative humidity, respectively, at room temperature. These moisture conditions were measured on the day of the test, which was at least one year after fabrication of the columns.

Type-K Chromel-alumel thermocouples, 0.91 mm thick, were installed at mid-height in the columns for measuring concrete and rebar temperatures at different locations in the cross-section. Full details on the design and fabrication of columns are given in Reference 7.

## Test Apparatus

The tests were carried out by exposing the columns to heat in a furnace specially built for testing loaded columns under fire conditions. The furnace consists of a steel framework supported by four steel columns, with the furnace chamber inside the framework. The test furnace was designed to produce conditions, such as temperature, structural loads and heat transfer, to which a member might be exposed during a fire. The furnace has a loading capacity of 1,000 t. Full details on the characteristics and instrumentation of the column furnace are provided in Reference 9.

### **Test Conditions and Procedure**

The columns were installed in the furnace by bolting the endplates to a loading head at the top and to a hydraulic jack at the bottom. The end conditions of the columns were fixed-fixed for all tests. For each column, the length exposed to fire was approximately 3000 mm. At high temperature, the stiffness of the unheated column ends, which is high in comparison to that of the heated portion of the column, contributes to a reduction in the column effective length. In previous studies, it was found that, for columns tested with fixed ends, an effective length of 2000 mm represents experimental behavior [10].

All columns were tested under concentric loads. Column THC4 was subjected to a load of 2000 kN, which is equal to 54% of the ultimate load according to ACI318 [3]. Column THC8 was subjected to a load of 2000 kN or 71% of the ultimate load, column THS11 to a load of 2200 kN or 66% of the ultimate load, and column THP14 to a load of 2200 kN or 67% of the ultimate load. The load intensity, defined as the ratio of the applied load to the column resistance for the various columns is given in Table 1.

The load was applied approximately 45 min before the start of the fire test and was maintained until a condition was reached at which no further increase of the axial deformation could be measured. This was selected as the initial condition for the axial deformation of the column. During the test, the column was exposed to heat, controlled in such a way that the average temperature in the furnace followed, as closely as possible, the ASTM E119-88 [11] or CAN/ULC-S101 [12] standard temperature-time curve. The load was maintained constant throughout the test. The columns were considered to have failed and the tests were terminated when the hydraulic jack, which has a maximum speed of 76 mm/min, could no longer maintain the load.

The main results from the experimental studies, aimed at validating the computer model, are presented in the following sections. Detailed results from the experimental studies, including measured temperatures and deflections, are described in Reference 7.

## **NUMERICAL MODEL**

### **Description of the Model**

A numerical model for predicting the behavior of HPC columns, exposed to fire, was developed as part of this study. The numerical procedure used in the model is similar to the one which was previously applied to the fire resistance calculations of NSC columns [13,14].

The fire resistance calculation is performed in three steps; namely, the calculation of the temperatures of the fire to which the column is exposed, the calculation of the temperatures in the column, and the calculation of the resulting deformations and strength, including an analysis of the stress

and strain distribution. In the strength analysis calculations, the extent of spalling is accounted for through a simplified approach. Detailed equations for the calculation of the column temperatures and strength are given in References 13 and 14.

### Fire Temperature

In the numerical model, it is assumed that the fire exposed surface area of the column is exposed to the heat of a fire, whose temperature follows that of the standard fire exposure described in ASTM E119-88 [11] or CAN/ULC S101 [12]. This temperature course can be approximated by the following expression:

$$T_f = 20 + 750[1 - \exp(-3.79553\sqrt{t})] + 170.41\sqrt{t} \quad (1)$$

where  $\tau$  is the time in hours and  $T_f$  is the fire temperature in °C at time  $\tau$ .

### Temperatures in Column

The column temperatures are calculated by a finite difference method [15]. Figure 1 shows the elevation and cross-sectional details of a typical RC column. The cross-sectional area of the column is subdivided into a number of elements, arranged in a triangular network (Figure 2). The elements are square inside the column and triangular at the column surface. For the inside elements, the temperature at the centre is taken as representative of the entire element. For the triangular surface elements, the representative points are located on the centre of each hypotenuse.

For reasons of symmetry, only one-quarter of the section needs to be considered when calculating the temperature distribution in columns with a rectangular cross-section.

The temperature rise in the column can be derived by creating a heat balance for each element. The calculations were carried out for a unit length of the column. As an illustration, for the elements at the surface of the column along the x-axis, the temperature at time  $t=(j+1)\Delta t$  is given by the expression:

$$T_{1,n}^{j+1} = T_{1,n}^j + \frac{2\Delta t}{[(r_c c_c)_{1,n}^j + r_w c_w f_{1,n}^j] (\Delta x)^2} \left\{ \left( \frac{k_{2,(n-1)}^j + k_{1,n}^j}{2} \right) (T_{2,(n-1)}^j - T_{1,n}^j) + \left( \frac{k_{2,(n+1)}^j + k_{1,n}^j}{2} \right) (T_{2,(n+1)}^j - T_{1,n}^j) + \sqrt{2} e_f e_c s \Delta x [(T_f^j + 273)^4 - (T_{1,n}^j + 273)^4] \right\} \quad (2)$$

Where  $T$  is the temperature in °C,  $\mathbf{r}$  is the density in kg/m<sup>3</sup>,  $c$  is the specific heat in J/kg°C,  $f$  is the concentration of moisture (fraction of volume),  $\Delta t$  is the increment of time,  $\Delta x$  is the width of mesh in meter,  $k$  is thermal conductivity in W/m°C,  $s$  is the Stefan-Boltzmann constant in W/m<sup>2</sup> K<sup>4</sup> and  $e$  is the emissivity. The subscripts  $c$ ,  $w$  and  $f$  represent concrete, water and fire, respectively. The subscripts  $m$ ,  $n$ , ( $M$ ,  $N$ ), represent points on the thermal network on inner (outer boundary) elements.

For the elements at the surface of the column along the y-axis, the temperature at the time  $t=(j+1)\Delta t$  is:

$$T_{m,N}^{j+1} = T_{m,N}^j + \frac{2\Delta t}{[(r_c c_c)_{m,N}^j + r_w c_w f_{m,N}^j] (\Delta x)^2} \left\{ \left( \frac{k_{(m-1),(N-1)}^j + k_{m,N}^j}{2} \right) (T_{(m-1),(N-1)}^j - T_{m,N}^j) + \right.$$

$$\left( \frac{k_{(m+1),(N-1)}^j + k_{m,N}^j}{2} \right) \left( T_{(m+1),(N-1)}^j - T_{m,N}^j \right) + \sqrt{2} \mathbf{e}_f \mathbf{e}_c \mathbf{s} \Delta \mathbf{x} \left[ (T_f^j + 273)^4 - (T_{m,N}^j + 273)^4 \right] \quad (3)$$

Similar expressions can be derived for elements in the concrete. By solving the heat balance equation for each layer, the temperature history of the column can be calculated, using the temperature-dependent thermal properties of the concrete and reinforcing steel.

The effect of moisture is taken into account by assuming that, in each element, the moisture starts to evaporate when the temperature of the element reaches 100°C. During the period of evaporation, all the heat supplied to an element is used for the evaporation of the moisture until the element is dry.

### Strength of Column

In order to calculate the strains and stresses in the column and its strength during fire exposure, the triangular network described above is transformed into a square network. In Figure 2, a quarter section of this network, consisting of square elements, arranged parallel to the  $x$ - and  $y$ -axis of the section, is shown. The arrangement of the elements in the three other quarter sections is identical. The temperatures, deformations and stresses in each element are represented by those at the centre of the element. The temperature at the centre of each element is obtained by averaging the temperatures of the elements in the triangular network noted above.

For the steel reinforcing bars, an approximate average bar temperature is obtained by considering the column as consisting entirely of concrete and selecting the temperature at the center of the bar section as the representative bar temperature. Temperature measurements at various locations during fire tests showed that the difference in temperature in the bar and sections are small [13].

The strain in an element of concrete can be given as the sum of the thermal expansion of the concrete, the axial strain due to compression and the strain due to bending of the column. A similar calculation is performed for the steel reinforcing bar elements.

The stresses at mid-section in the concrete elements can be calculated for any value of the axial strain,  $\epsilon$ , and curvature,  $1/\rho$ . From these stresses, the load that each element carries and its contribution to the internal moment at mid-section can be determined. By adding the loads and moments, the load that the column carries and the total internal moment at mid-section can be calculated. Detailed equations for strength calculation are derived in References 13 and 14.

The fire resistance of the column is derived by calculating the strength, i.e., the maximum load that the column can carry, at several consecutive times during the exposure to fire.

### Extent of Spalling

Spalling of concrete under fire conditions is one of the major concerns in HSC and should be accounted for in modeling the behavior of HSC columns exposed to fire. Spalling is a complex phenomenon and there is still a debate on the exact mechanism for the occurrence of spalling [8]. Data from various studies show that spalling in HSC is affected by concrete strength, concrete density, load intensity and type, moisture content, tie configuration, fire intensity, aggregate type, addition of fibers and specimen dimensions [8]. For accurate modeling of spalling, pore pressure-temperature relationship is required. However, such data is not available at present. Hence a simplified approach is used in order to minimize the complexity of the model and to facilitate easy usage of the computer program.

Based on detailed experimental studies on HSC columns, it was found that spalling occurs when temperatures in concrete reach above 350°C [7]. This is shown in Figure 3, which shows temperatures

at various time intervals and the initiation of spalling, as observed during fire resistance test of column THC4. It can be seen from Figure 3, at about 15 minutes the temperatures close to the column surface (at depths much less than 19.5 mm) reaches 350°C, and spalling is likely to occur in this zone. At about 30 minutes the spalling zone spreads to about 19.5 mm from surface. Data from the experimental studies also showed that, while spalling occurs throughout the cross-section in the case of columns with straight ties, spalling occurs only outside the reinforcement core when the ties are bent in to the concrete core [5]. Further, the presence of steel or polypropylene fibers and the type of aggregate in concrete influence the extent of spalling [7]. The addition of fibers to concrete helps in minimising the extent of spalling in HSC members [8].

Based on the above observations, the following guidelines were incorporated into the model to determine the extent of spalling.

1. Spalling occurs when the temperatures in an element exceed 350°C.
2. Spalling is influenced by the tie configuration adopted for the column.
  - Spalling occurs throughout the cross-section when the ties are bent in a conventional pattern.
  - Spalling occurs only outside the reinforcement cage when the ties are bent at 135° into the concrete core (as shown in Figure 4).
3. The extent of spalling is dependent on the type of aggregate, presence of fiber reinforcement and spacing of ties.
  - The extent of spalling is higher (100%) in the siliceous aggregate HSC than that for carbonate aggregate HSC (40%).
  - No spalling occurs when polypropylene fibers are present in the concrete mix.
  - The extent of spalling in HPC columns with steel fiber is about 50%.
  - No spalling occurs inside the reinforcement core when the tie spacing is 0.7 times the standard spacing.
  - The extent of spalling is also influenced by relative humidity. A higher relative humidity in the HPC column (90% or higher) leads to higher spalling.

The above guideline have been incorporated into the computer program and the user can select the extent of spalling based on the design parameters. These sets of rules are checked for each element of the network shown in Figure 2. As an illustration, when the temperature exceeds 350°C, spalling is said to occur in that element, and the contribution of that element to strength is zero.

### **Assumptions**

The following assumptions are made in the strength calculations:

1. The curvature of the column varies from pin ends to mid-height according to a straight-line relation.
2. Plane sections remain plane.
3. Concrete has no tensile strength.
4. There is no slip between steel and concrete.
5. The reduction in column length before exposure to fire, consisting of free shrinkage of the concrete, creep, and shortening of the column due to load, is negligible. This reduction can be eliminated by selecting the length of the shortened column as the initial length from which the changes during exposure to fire are determined.
6. The contribution of any element to strength depends on the extent of spalling in that element.

Based on the above assumptions, the column strength during exposure to fire was calculated. In the calculations, the network of elements shown in Figure 2 was used. Because the strains and stresses in the elements are not symmetrical with respect to the y-axis, the calculations were performed for both the network shown and for an identical network to the left of the y-axis. The load that the column can carry and the moments in the section were obtained by adding the loads carried by each element and the moments contributed by them.

## COMPUTER IMPLEMENTATION

### Computer Program

The numerical procedure described above was incorporated into a computer program, written in the Fortran language. Figure 5 shows a flow chart of the calculation procedure associated with the computer program. For any time step, the analysis starts with the calculation of temperatures due to fire. The next stage is to determine the cross-sectional temperatures by making use of the thermal properties of the column materials. In the third stage, the strength of the column, during exposure to fire, is determined by successive iterations of the axial strain and curvature until the internal moment at mid-height is in equilibrium with the applied moment. The extent of spalling in the section is accounted for based on the above set of guidelines.

For any given curvature and, therefore for any given deflection at mid-height, the axial strain is varied until the internal moment at the mid-section is in equilibrium with the applied moment given by the product:

$$\text{load} \times (\text{deflection} + \text{eccentricity})$$

In this way, a load deflection curve can be calculated for specific times during the exposure to fire. From these curves, the strength of the column, i.e., the maximum load that the column can carry, can be determined for each time step. When the equilibrium condition is satisfied, the iteration for curvature is continued in order to make sure that the point at which the equilibrium is achieved corresponds to the maximum load condition.

The fire resistance of the column is derived by calculating the strength of the column as a function of the time of exposure to fire. This strength reduces gradually with time. The time increments continue until a certain point at which the strength becomes so low that it is no longer sufficient to support the load. At this point, the column becomes unstable and is assumed to have failed. The time to reach this failure point is the fire resistance of the column.

### Idealisation

For thermal and mechanical analysis of RC columns, the cross-section of the column is idealised as a network of elements. Figure 2 shows typical idealisations for the thermal and mechanical analyses, respectively. The mesh size selected in the input file corresponds to the mesh size ( $\Delta x$ ) in the triangular network (Figure 2). The program automatically determines the number of elements, based on the mesh size specified in the input data. Alternatively, for a desired number of concrete elements, the mesh size can be calculated as:

$$\Delta e = \frac{b}{\sqrt{2} * N} \quad (4)$$

where N is the number of elements along the x axis and b is the breadth of the column.

The program allows for six different symmetric rebar configurations. The inputs required are the configuration number, the concrete cover and the radius of the rebars. From this information and the geometrical shape of the idealized rebar configurations, the locations of the reinforcement bars within the column cross-section are calculated.

The computer program is developed to account for axial loads and bending moments. In cases where only axial loads are present, to facilitate the strength calculation, a small, finite value of initial eccentricity is assumed in the analysis.

### **Material properties**

*Concrete:* The fire resistance behavior of HPC columns is influenced by the concrete strength and the type of aggregate present in the concrete. The user has the option of selecting either NSC or HSC and siliceous aggregate concrete or carbonate aggregate concrete. Relevant formulas for the thermal and mechanical properties of concrete as a function of temperature in the range of 0-1000°C, are given in the Appendix for HPC made of siliceous and carbonate aggregate [16,17]. The stress-strain curves for the concrete, expressed as a function of temperature are built into the computer program. While the presence of fibers has little influence on the thermal properties, they may have some influence on the mechanical and deformation properties. However, due to lack of data of these properties for fiber reinforced HPC, the program uses the properties of HSC for all HPC columns. Also, no sensitivity analysis is carried out on the effect of variation of material properties on fire resistance.

In the input data file, the user has to specify the 28-day compressive (design) strength of concrete, the initial moisture content in the concrete and the type of aggregate in the concrete. The initial moisture content of the column is expressed as the volume of water per cubic meter of concrete.

*Steel Reinforcement:* Similar to concrete, the thermal and mechanical properties of reinforcing steel are incorporated into the program and are given in the ASCE Manual [18]. The stress-strain curves for reinforcing steel are expressed as a function of temperature and are given in the Appendix. The only material property the user has to specify, within the data file, is the yield strength of the reinforcement bars.

*Water:* The values of the thermal capacity of water and the heat of vaporization, which are used in calculating the moisture vaporization when the temperature reaches 100°C, are also built into the computer program.

### **Input Description**

The basic input for the program consists of the structural geometry, cross-sectional properties, material properties, loading characteristics, spalling parameters and general data such as the time increments, maximum time limit, and emissivity characteristics of the fire. The user has to specify the print codes for obtaining detailed or abbreviated results from the analysis.

As part of the loading data, the applied load on the column and a small value for assumed eccentricity are to be specified. The start time, time limit and the number of printouts per hour for the analysis must be entered into the input file.

The input data file is set up such that it is self-explanatory. The sequential order of the input must be strictly adhered to and consistent units must be used throughout.

### **Output Results**

The output from the program includes an echo of the input data and the results from the thermal and strength analysis. At each incremental time step, the strength, axial deformation and lateral deflection of the column are given. The temperature distribution, loads and moments, and the stress-strain distribution across the column cross-section are also given for each time step. The fire resistance of the RC column, corresponding to an applied load level, is also written to the file.

## RESULTS AND DISCUSSION

Using the numerical model described in this paper, the temperatures, the axial deformations and the fire resistance were calculated for the four HPC columns given in Table 1. In the calculations, the thermal and mechanical properties of the concrete and steel, given in the Appendix, were used.

The results obtained from the computer program can be used to trace the response of an RC column from the initial pre-loading stage to collapse. In the following, calculated temperatures and axial deformations of the columns will be compared with the measured temperatures and axial deformations from full-scale fire resistance tests of HPC columns THC4 and THS11. RC columns THC4 and THC 8 are made of plain HSC, while RC column THS11 and THP14 are made of steel and polypropylene fiber reinforced HSC.

### Temperatures History

In Figure 6, calculated temperatures are compared with those measured at various depths for the four columns. It can be seen that there is good agreement between calculated and measured temperatures. The temperatures measured at the center of the columns initially show a relatively rapid rise in temperature, followed by a period of nearly constant temperatures in the early stages of the test. This temperature behavior may be the result of thermally-induced migration of moisture towards the center of the column where, as shown in the figures, the influence of migration is most pronounced [13]. Although the model takes into account evaporation of moisture, it does not take into account the migration of the moisture towards the center. That migration appears to account for the deviation between calculated and measured temperatures at the earlier stages of fire exposure. At later stages, which are important from the point of view of predicting fire resistance of columns, there is good agreement between calculated and measured temperatures.

### Axial Deformations

In Figure 7, the calculated and measured axial deformations are shown for columns THC4, THC8, THS11 and THP14. It can be seen that the computer model predicts reasonably well, the trend in the progression of the axial deformations with time. However, the variation between predicted and measured deformations could be partly attributed to the “spalling factor” assumed in the analysis, since the extent of spalling used in the analysis has a moderate influence on the axial deformations. To illustrate the sensitivity of the extent of spalling on axial deformations, the analysis was carried out for two cases for column THC4, namely, with 100% spalling and with 50% spalling. It can be seen in Figure 6(a) that the difference between the predicted and measured deformations reduces considerably when a 50% spalling factor is assumed. For this column the extent of spalling, to the cover concrete, was about 40% in the fire resistance test.

The difference between calculated and measured axial deformations at the expansion stage are on the order of 2 mm, which may be regarded as small compared to the length of the column of about 3800 mm. For column THC4, in the descending portion of the axial deformation curve, the predicted deformations are larger than the measured deformations and this could again be attributed to the conservative assumption of higher “spalling factor”. As can be seen in the figure, when the spalling factor of 50% is assured the difference between measured and predicted deformation is reduced.

In column THS11, the presence of steel fibers has some influence of mechanical and deformation properties and this could not be accounted for in the analysis due to lack of data on material properties of fiber reinforced HPC at an elevated temperature. Further, it must also be noted that the columns deform axially as a result of several factors, namely, load, thermal expansion, bending and the effect of creep, which is significant in later stages of fire exposure and cannot be completely taken into account in the calculations. The axial deformation predictions for columns THC8 and THP14 followed a similar trend.

### **Fire Resistance**

The measured and predicted fire resistances of four HPC columns are compared in Table 1. The time to reach failure is defined as the fire resistance for the column. For plain HSC columns, THC4 and THC8, the measured fire resistances were 202 and 305 minutes, while the predicted fire resistances were 186 and 271 minutes, respectively. The predicted fire resistances are within 10% of the measured values, thus indicating that the predictions from the model are conservative.

For column THS11 the measured fire resistance was 206 min while the predicted fire resistance was 176 minutes. This high variation could be attributed to the contribution of steel fiber to strength that is not accounted for in the model. For column THP14 the measured and calculated fire resistances were 233 and 183 minutes, respectively. In this column also the presence of polypropylene fibers also provided confinement to the section and enhanced fire resistance slightly. This could not be accounted for in the model due to the lack of data on the properties of fiber reinforced HPC at elevated temperature.

In all columns most of the spalling occurred outside the reinforcing core (cover concrete) due to ties being bent at 135° in to the concrete core (as shown in Figure 4). Further, the presence of steel or polypropylene fibers and the type of aggregate in concrete influence the extent of spalling [7]. The spalling was highest in column THC4 which was made with siliceous aggregate. The presence of carbonate aggregate helped in minimising spalling in column THC8. In column THS11 the extent of spalling was about 40%, while in the case of THP14, with polypropylene fibers, the spalling was minimum (about 15%). Full details on spalling in these columns are given in Reference 7.

The predicted fire resistance from the computer program is within 10% of the measured value for plain HPC and within 20% for fibre reinforced HPC column and this is adequate for practical purposes. The larger variation between predicted and measured fire resistance is due to the use of conservative spalling factor and also due to not accounting for the contribution of fibres to strength. The accuracy of the predictions from the model can be enhanced, in future, provided the relevant material properties of fibre reinforced HPC are incorporated in to the model.

### **CONCLUSIONS**

Based on the results of this study, the following conclusions can be drawn:

1. The computer program presented in this study is capable of predicting the fire resistance of HPC columns, within the limitations of the basic test parameters, with an accuracy that is adequate for practical purposes.
2. The numerical model accounts for spalling of HPC under fire conditions. The simplified approach used for calculating spalling accounts for tie configuration, aggregate type and presence of fibers.
3. Using the model, the fire resistance of HPC columns can be evaluated for any value of the significant parameters, such as load, section dimensions, column length, concrete strength, aggregate type and fiber reinforcement, without the necessity of testing.

4. The model can also be used for the calculation of the fire resistance of columns made with concrete other than those investigated in this study; for example, lightweight aggregate concrete or rectangular cross-section, if the relevant material properties are known.
5. Data on the mechanical and deformation properties of fiber reinforced HPC, at elevated temperatures, is needed for more accurately predicting the fire resistance of HPC columns.

#### **ACKNOWLEDGEMENTS**

The research presented in this paper is the result of partnership between the National Research Council of Canada and National Chiao Tung University, Taiwan. The authors would like to thank the National Research Council of Canada and ABRI of Interior Department, Taiwan for their financial support.

## REFERENCE

1. National Building Code of Canada 1995. National Research Council of Canada, Ottawa, ON.
2. Canadian Standards Association, Code for the Design of Concrete Structures for Buildings. CAN3-A23.3-M94, Rexdale, ON, 1994.
3. ACI Committee 318, "Building Code Requirements for Reinforced Concrete" (ACI 318-95), American Concrete Institute, Detroit, 1995.
4. Diederichs, U., Jumppanen, U.M. and Schneider, U., High Temperature Properties and Spalling Behaviour of High Strength Concrete. Proceedings of Fourth Weimar Workshop on High Performance Concrete, HAB Weimar, Germany, pp. 219-235, 1995.
5. Kodur, V.K.R. and McGrath, R., Performance of High Strength Concrete Columns under Severe Fire Conditions. Proceedings Third International Conference on Concrete under Severe Conditions, Vancouver, BC, Canada, pp. 254-268, 2001.
6. Phan, L.T., Fire Performance of High-Strength Concrete: A Report of the State-of-the-Art. National Institute of Standards and Technology, Gaithersburg, MD, 1996.
7. Kodur, V.K.R., Cheng, F.P. and Wang T.C., Effect of Strength and Fiber Reinforcement on the Fire Resistance of High Strength Concrete Columns, ASCE, Journal of Structural Engineering, 129(2), pp. 1-22, 2003.
8. Kodur, V.K.R., "Spalling in High Strength Concrete Exposed to Fire - Concerns, Causes, Critical Parameters and Cures", Proceedings: ASCE Structures Congress, 1-8, Philadelphia, U.S.A., 2000.
9. Lie, T. T., New Facility to Determine Fire Resistance of Columns. Canadian Journal of Civil Engineering, Vol. 7, No. 3, pp. 551-558, 1980.
10. Lie, T. T., and Woollerton, J. L., Fire Resistance of Reinforced Concrete Columns: Test Results. Institute for Research in Construction Internal Report No. 569, National Research Council of Canada, Ottawa, ON, 302 pp, 1988.
11. American Society for Testing and Materials, Standard Methods of Fire Endurance Tests of Building Construction and Materials. ASTM E119-88, Philadelphia, PA, 1990.
12. Underwriters' Laboratories of Canada, Standard Methods of Fire Endurance Tests of Building Construction and Materials". CAN/ULC-S101-M89, Scarborough, ON, 49 pp., 1989.
13. Lie, T.T and Irwin, R.J. 1993. Method to Calculate the Fire Resistance of Reinforced Concrete Columns with Rectangular Cross Section. ACI Structural Journal (90) 1, 52-60.
14. Kodur, V.K.R. and Lie, T.T., A Computer Program to Calculate the Fire Resistance of Rectangular Reinforced Concrete Columns. Third Canadian Conference on Computing in Civil and Building Engineering, Ottawa, Canada, 1996, pp. 11-20, 1996.
15. Dusinberre, G. M., *Heat Transfer Calculations by Finite Differences*, International Textbook Company, Scranton, 1961, 293 pp.
16. Kodur, V.K.R. and Mohamed Sultan, Thermal Properties of High Strength Concrete at Elevated Temperatures. CANMET-ACI-JCI International Conference on Recent Advances in Concrete Technology, pp. 467-480, Tokushima, Japan, June 1998.
17. Cheng, F.P., Kodur, V.K.R. and Wang T.C., Stress-strain Curves for High Strength Concrete at Elevated Temperatures, submitted to ASCE, Journal of Structural Engineering.
18. Lie, T.T., Ed. 1992. Structural Fire Protection, Manuals and Reports on Engineering Practice, No. 78. ASCE, New York, NY.

## Appendix – Properties of HSC

### A.1 Stress–Strain Relationships

$$\text{For } e_c \leq e_{\max} \quad f_c = f'_c \left[ 1 - \left( \frac{e_{\max} - e_c}{e_{\max}} \right)^H \right]$$

$$\text{Where } H = 2.28 - 0.12 f'_{co}$$

$$e_{\max} = 0.018 + (6.7 f'_{co} + 6T + 0.03T^2) \times 10^{-6}$$

$$\text{For } e_c > e_{\max} \quad f_c = f'_c \left[ 1 - \left( \frac{30(e_c - e_{\max})}{(130 - f'_{co})e_{\max}} \right)^2 \right]$$

$$\text{For } T < 100^\circ\text{C} \quad f'_c = f'_{co} [1.0625 - 0.003125 (T - 20)]$$

$$\text{For } 100 \leq T < 400^\circ\text{C} \quad f'_c = 0.75 f'_{co}$$

$$\text{For } T \geq 400^\circ\text{C} \quad f'_c = f'_{co} (1.33 - 0.00145 T)$$

$$\text{Such that: } 0 \leq f'_c \leq f'_{co}$$

Unit: MPa

### A.2 Thermal Capacity (J/m<sup>3</sup> °C)

*Siliceous Aggregate concrete*

|                                       |   |
|---------------------------------------|---|
| for $0 \leq T \leq 200^\circ\text{C}$ | $\rho_c c_c = (0.005T + 1.7) \times 10^6$   |
| for $200 < T \leq 400^\circ\text{C}$  | $\rho_c c_c = 2.7 \times 10^6$              |
| for $400 < T \leq 500^\circ\text{C}$  | $\rho_c c_c = (0.013T - 2.5) \times 10^6$   |
| for $500 < T \leq 600^\circ\text{C}$  | $\rho_c c_c = (-0.013T + 10.5) \times 10^6$ |
| for $T > 600^\circ\text{C}$           | $\rho_c c_c = 2.7 \times 10^6$              |

*Carbonate Aggregate concrete*

|                                       |   |
|---------------------------------------|---|
| for $0 \leq T \leq 400^\circ\text{C}$ | $\rho_c c_c = 2.45 \times 10^6$               |
| for $400 < T \leq 475^\circ\text{C}$  | $\rho_c c_c = (0.026T - 12.85) \times 10^6$   |
| for $475 < T \leq 650^\circ\text{C}$  | $\rho_c c_c = (0.0143T - 6.295) \times 10^6$  |
| for $650 < T \leq 735^\circ\text{C}$  | $\rho_c c_c = (0.1894T - 120.11) \times 10^6$ |
| for $735 < T \leq 800^\circ\text{C}$  | $\rho_c c_c = (-0.263T + 212.4) \times 10^6$  |
| for $800 < T \leq 1000^\circ\text{C}$ | $\rho_c c_c = 2 \times 10^6$                  |

### A.3 Thermal Conductivity (W/m °C)

*Siliceous Aggregate concrete*

$$0 \leq T \leq 1000^\circ\text{C} \quad k_c = (2 - 0.0011T) \times 0.85$$

*Carbonate Aggregate concrete*

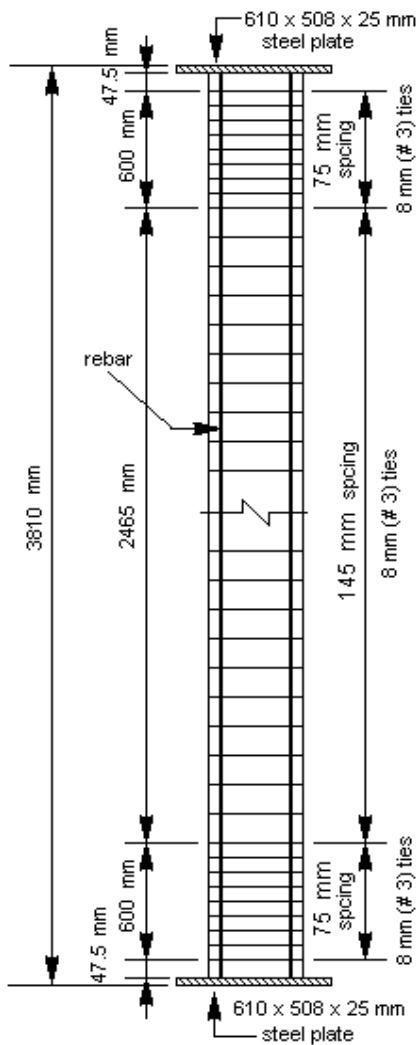
$$0 \leq T \leq 300^\circ\text{C} \quad k_c = (2 - 0.0013T) \times 0.85$$

$$300 < T \leq 1000^\circ\text{C} \quad k_c = (2.21 - 0.002T) \times 0.85$$

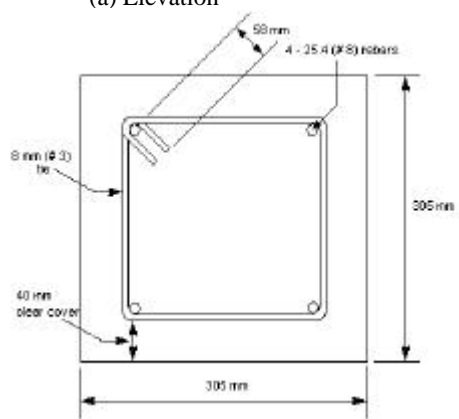
### A.4 Thermal Expansion (m/m °C)

(siliceous and carbonate aggregate concretes)

$$a = (0.008 T + 6) \times 10^{-6}$$

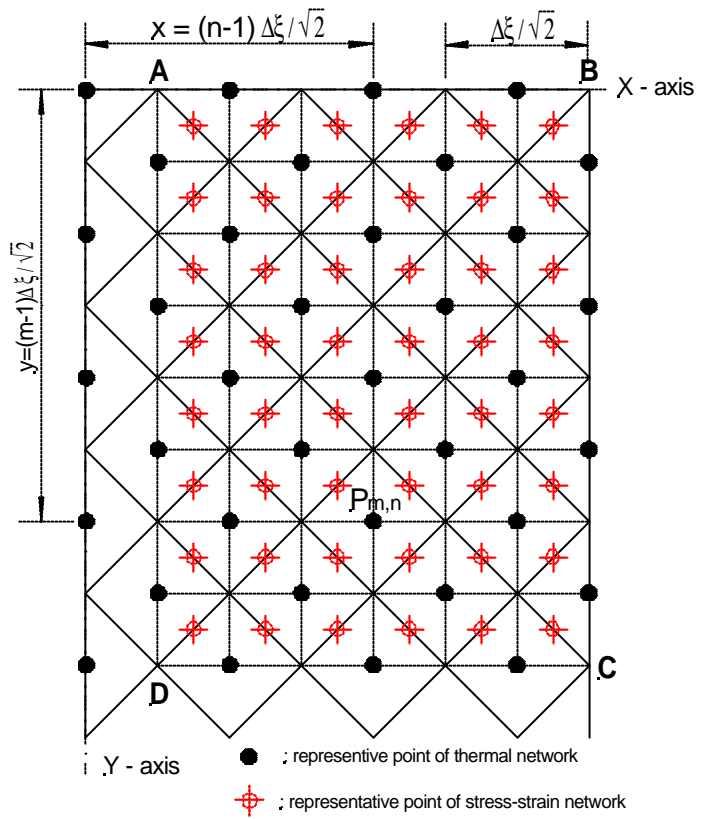


(a) Elevation

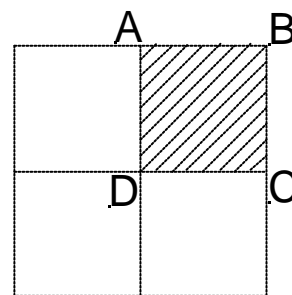


(b) Cross section

Figure 1 Elevation and cross-section of reinforced concrete columns



(a) Quarter section



(b) Full cross section

Figure 2 Thermal and stress-strain network in one-quarter cross section

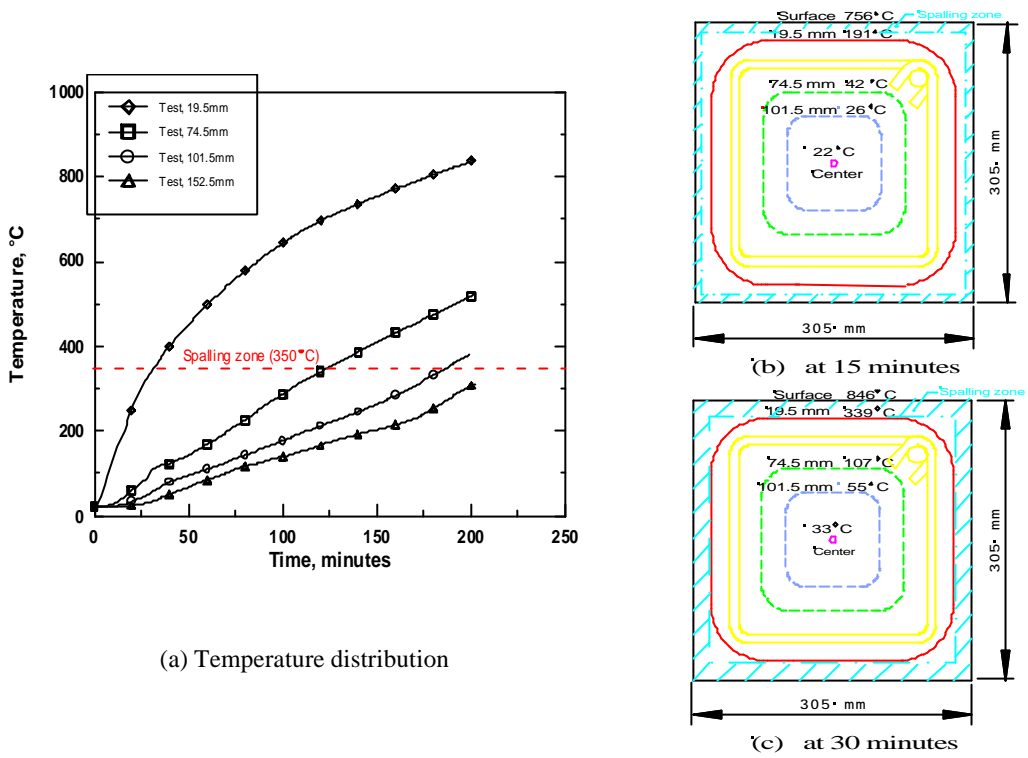
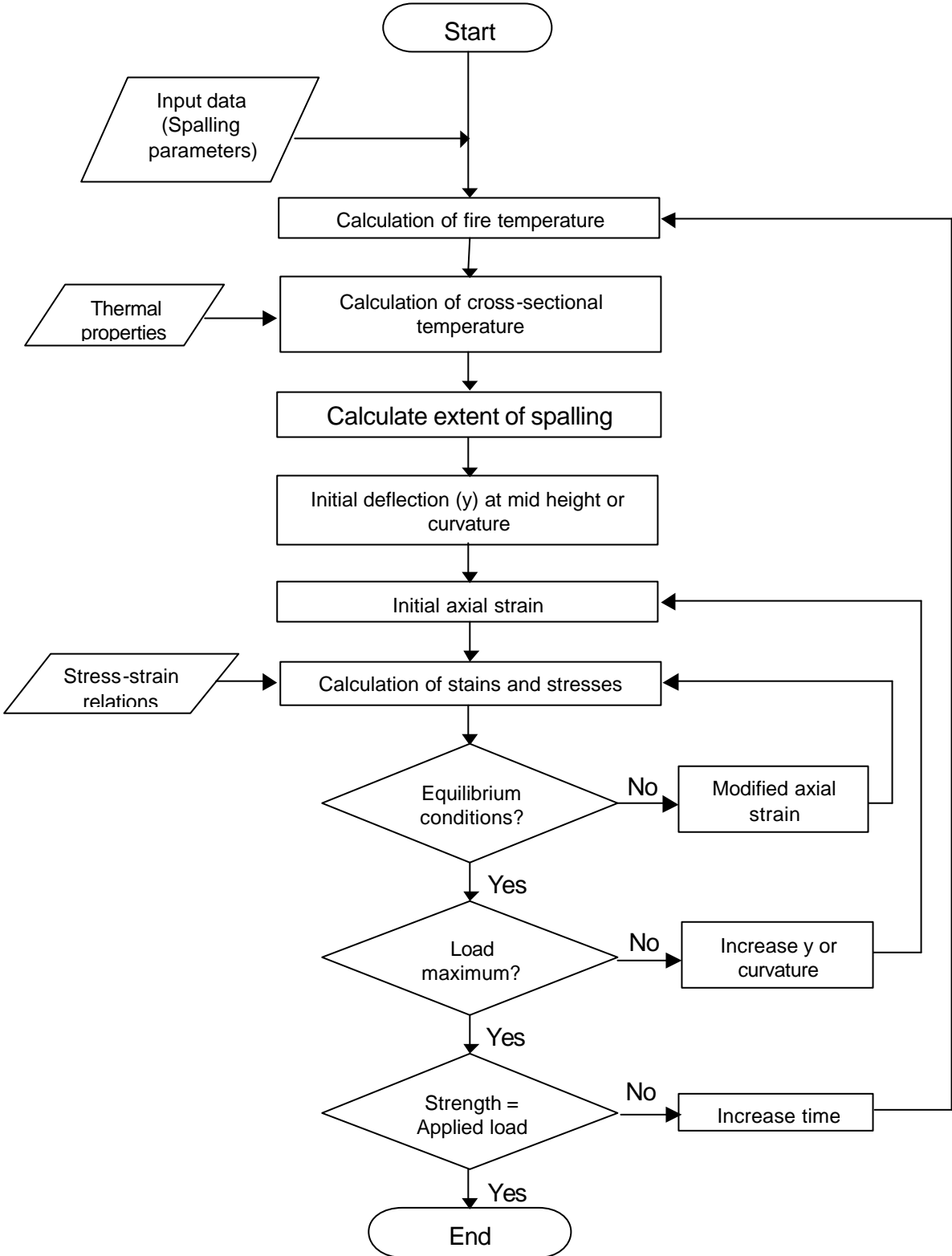


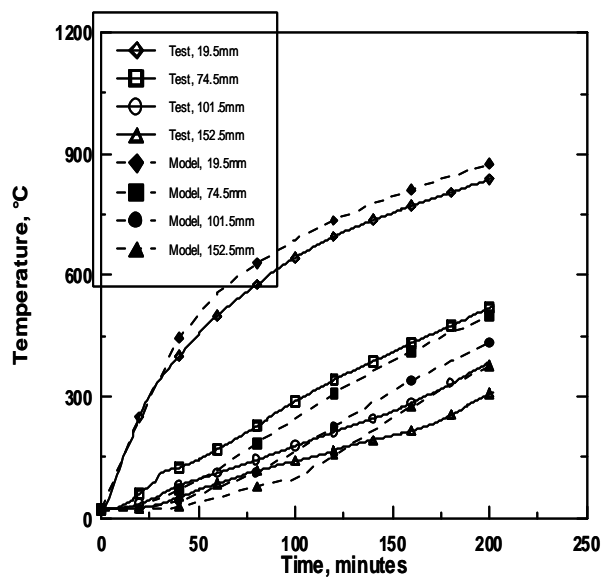
Figure 3 Temperature profiles for column THC4 at various depths and at various time intervals



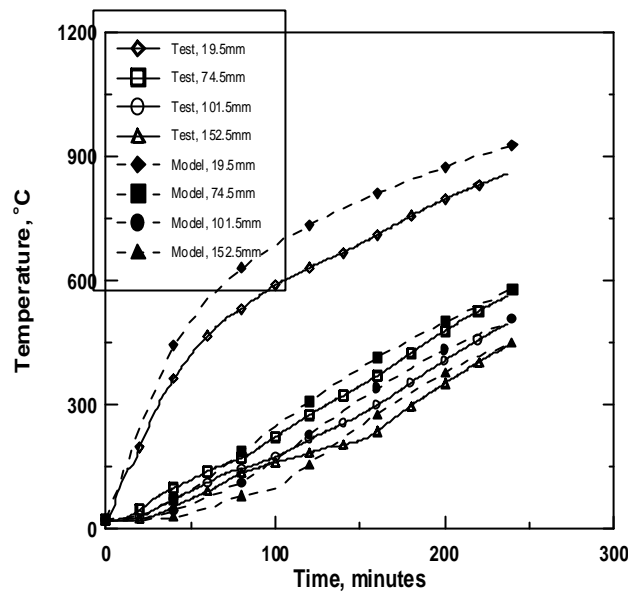
Fig. 4 Conventional and Modified Tie Configuration for Reinforced Concrete Column

Figure 5 Flowchart showing the numerical procedure for fire resistance calculations

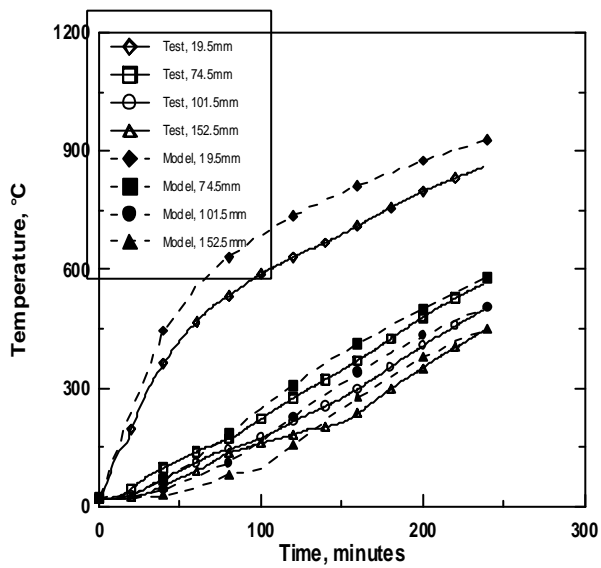




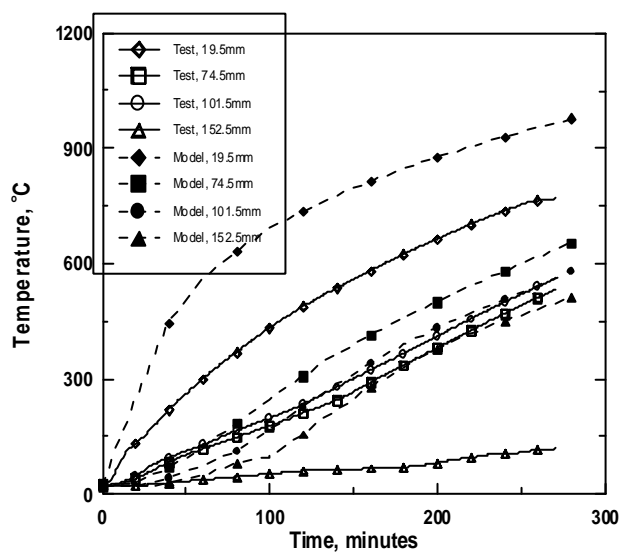
(a) Column THC4



(b) Column THC8

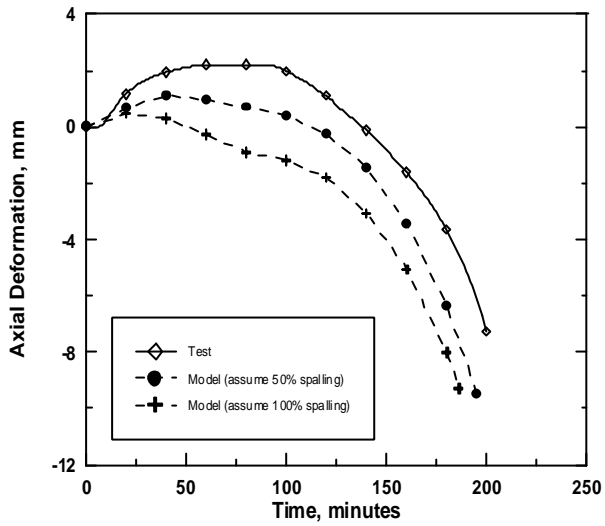


(c) Column THS11

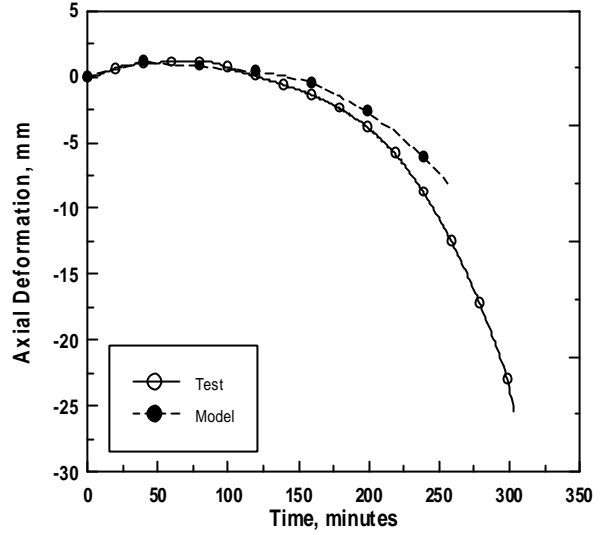


(d) Column THP14

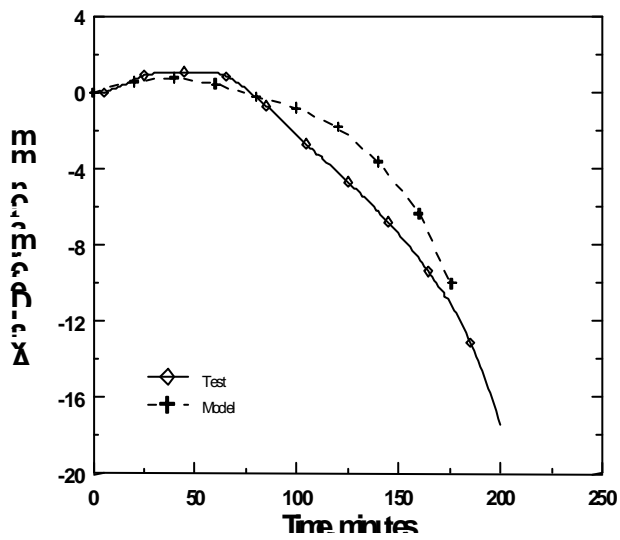
Figure 6 Comparison of temperature distribution at various depths for HPC columns



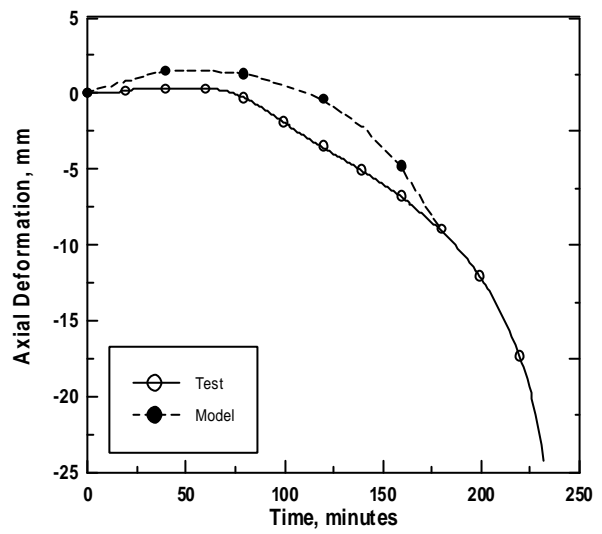
(a) Column THC4



(b) Column THC8



(c) Column THS11



(d) Column THP14

Figure 7 Comparison of axial deformation for HPC columns